Serial correlation in neural spike trains: Experimental evidence, stochastic modeling, and single neuron variability

Farzad Farkhooi, Martin F. Strube-Bloss, and Martin P. Nawrot[*]

*Neuroinformatics & Theoretical Neuroscience, Institute of Biology-Neurobiology, Freie Universität Berlin
and Bernstein Center for Computational Neuroscience Berlin, Germany*

The activity of spiking neurons is frequently described by renewal point process models that assume the statistical independence and identical distribution of the intervals between action potentials. However, the assumption of independent intervals must be questioned for many different types of neurons. We review experimental studies that reported the feature of a negative serial correlation of neighboring intervals, commonly observed in neurons in the sensory periphery as well as in central neurons, notably in the mammalian cortex. In our experiments we observed the same short-lived negative serial dependence of intervals in the spontaneous activity of mushroom body extrinsic neurons in the honeybee. To model serial interval correlations of arbitrary lags, we suggest a family of autoregressive point processes. Its marginal interval distribution is described by the generalized gamma model, which includes as special cases the log-normal and gamma distributions, which have been widely used to characterize regular spiking neurons. In numeric simulations we investigated how serial correlation affects the variance of the neural spike count. We show that the experimentally confirmed negative correlation reduces single-neuron variability, as quantified by the Fano factor, by up to 50%, which favors the transmission of a rate code. We argue that the feature of a negative serial correlation is likely to be common to the class of spike-frequency-adapting neurons and that it might have been largely overlooked in extracellular single-unit recordings due to spike sorting errors.

I. INTRODUCTION

Stochastic point process models have a long tradition in cellular neurophysiology as a means to describe the random nature of action potential generation in spiking neurons [1–7]. The mathematical definition of a point process allows one to analytically calculate the distribution or the expectation value of a given stochastic variable and to formulate statistical predictions for experimental results. Numeric simulation of point processes is highly efficient and can be used to numerically construct distributions of stochastic variables that are analytically intractable. The class of renewal point processes [8] has gained particular popularity in theoretical neuroscience [2,4–7]. In a renewal model the intervals between successive events are independent and identically distributed. Thus, a renewal process is fully characterized by the distribution of interevent intervals. Selection of the specific model distribution allows one to incorporate some important physiological characteristics of spiking neurons such as an absolute and relative refractory period [6,7,9]. In the intact nervous system spiking neurons modulate their firing rate with time as a means of dynamic stimulus encoding and information processing. Point process models of neuronal spiking that follow a dynamic firing rate can be achieved with inhomogeneous variants of the renewal model where the process intensity follows a deterministic and explicitly time-dependent function. [9–15].

In the renewal model the probability for the occurrence of the ith spike at time t depends solely on the process intensity and the time that elapsed since the last spike $i-1$ at time

$T_{i-1} < t$, but there is no serial dependence on the previous history of spiking. However, several types of neurons in different systems have been shown to violate the renewal assumption of independent intervals in their spontaneous activity. The common feature of these neurons is a short-lived negative serial correlation of their interspike intervals (ISIs), which is likely to be a general property of neurons that feature a physiological mechanism of spike frequency adaptation (see Discussion).

In this paper we propose a class of autoregressive point-process models that incorporate serial correlation of interevent intervals for arbitrary serial correlation orders. Our model describes the marginal interevent interval distribution by the generalized gamma distribution which includes as special cases the log-normal, the gamma, the exponential, and the Weibull distributions. We derive expressions for the most relevant empiric measures of the interval statistics and perform maximum-likelihood estimates of the model parameters in our data set. Using physiologically plausible model parameters, we investigate the effect of a negative serial correlation on the variability of single-neuron discharge.

II. SERIAL INTERVAL CORRELATION IN DIFFERENT NEURAL SYSTEMS

The phenomenon of a significant negative serial interval correlation of order 1—i.e., the anticorrelation of neighboring intervals—is a common property of spiking neurons in various systems. In the sensory periphery this has been observed in the electrosensory *P*-type receptor of weakly electric fish [16,17], in the sensory ganglion receptors of paddle fish [18], and in the ganglion cells in the retina of goldfish [19] and cats [20,21]. In central parts of the mammalian

---

*Corresponding author: nawrot@neurobiologie.fu-berlin.de

TABLE I. Reports on negative first-order serial interval correlation in different preparations and cell types.

Ref.	Model system and neuron type	SC[a]
[16]	Weakly electric fish, isolated *P*-type receptors afferent	−0.52
[17]	Weakly electric fish, isolated *P*-type receptors afferent	−0.35
[26]	Weakly electric fish, electrosensory line lobe, pyramidal cells *in vivo*	−0.29
[18]	Paddle fish, sensory ganglion	~−0.4
[27]	Cat splanchnic, and hypogastric nerves *in vivo*	−0.3
[19]	Goldfish retina, ganglion cells *in vivo*	−0.13
[21]	Cat retina, ganglion cells *in vivo*	−0.06
[20]	Cat retina, ganglion cells *in vivo*	−0.17
[22]	Cat lateral superior olive *in vivo*	−0.2
[24]	Rat somatosensory cortex (*S*1) *in vivo*, regular spiking cells	−0.21
[24]	Rat somatosensory cortex (*S*1) *in vitro*, pyramidal cells	−0.07
[25]	Rat medial entorhinal cortex *in vitro* layer II stellate and layer III pyramidal neurons	$[-0.1, -0.4]$[b]
III[c]	Honeybee central brain *in vivo* mushroom body extrinsic neurons	−0.15

[a]SC: serial correlation coefficient; for the estimation method, refer to the respective reference.
[b]This study reported a rate dependent serial correlation.
[c]Refer to Sec. III.

brain, the same serial statistics has been reported for brain stem neurons in the lateral superior olive [22], in primate somatosensory cortex [23], and more recently in rat cortical neurons *in vivo* [24] and *in vitro* [24,25]. In the present paper we report the existence of the same type of short-lived serial dependence of ISIs for a class of central neurons in the mushroom body of the insect brain (cf. Sec. III). In Table I we summarized all quantitative accounts of a negative serial correlation.

III. EXPERIMENTAL RESULTS

We investigated the serial dependences of ISIs in the spontaneous activity of extrinsic neurons in the mushroom body (MB) of the honeybee. The mushroom body is known to play a significant role in learning and memory of insects [28]. The extrinsic neurons constitute the readout of the MB, and each cell receives converging input from thousands of MB Kenyon cells and, thereby, typically integrates different sensory modalities. Details of the *in vivo* preparation and the extracellular recording technique are described elsewhere [29,30]. In brief, we manufactured electrodes with three closely spaced polyurethane-coated copper wires (14 μm in diameter). The electrodes were inserted into the ventral part of the α lobe close to the peduncle, targeting the mushroom body extrinsic neurons, in particular the clusters *A*1, *A*2, *A*4,

*A*5, and *A*7 [31]. Raw signals were measured differentially from all three electrode pairs and bandpass filtered at 1–9 kHz using a Lynx-8 amplifier (Neuralynx, Tucson, AZ) before analog-to-digital (A/D) conversion with a sampling frequency of 20 kHz. Semiautomatic spike sorting was performed to identify the activity of up to three single units using Spike2 software (Cambridge Electronic Design, Cambridge, UK). In order to minimize the inference of potential spike sorting errors with our statistical estimates (see Discussion), we considered for each animal ($N=23$) only the unit that expressed the highest amplitude of the extracellular spike wave form.

Neural activity was measured under spontaneous conditions—i.e., when the animal was shielded from any sensory stimuli—for up to 20 min. Although the experimental condition was controlled, single-neuron activity could undergo short episodes with spontaneous modulation of its spike frequency, sometimes in parallel to a spontaneous motor behavior. Such overt changes of the firing rate, however, may severely compromise the statistical analysis of the ISIs [32]. Thus, in a first step of our analysis we identified in each data set the longest part of stationary activity. To this end, we measured the spike count in successive time bins of a fix length of either 1 s or 500 ms for a lower ($<10/s$) or higher firing rate, respectively, and divided the total series of counts into equal parts of 30 bins. Each subseries of the counting process was then tested for stationarity. We adopt the notion of weak stationarity of a time series [33], which requires three conditions to be fullfilled: The series must have (i) a constant mean, (ii) a finite variance, and (iii) its autocovariance must be translation invariant for an arbitrary time lag. Next, we performed the *Phillips Perron unit root test* (PP test), which is explained in detail elsewhere [34]. Briefly, the family of unit root tests estimates the likelihood of a random walk behavior. The random walk is a linear nonstationary time series. The PP test formulates the null hypothesis: The time series has a unit root; i.e., the time series is *not* stationary. If for a given count series the deviation from nonstationarity was significant ($P<0.1$), we considered it as stationary. Thereafter, subsequent stationary parts were pooled and the test was repeatedly performed until the longest stationary part was found. We used the PP.TEST function of the TSERIES package in the *R statistical environment* to perform this test. The truncation lag parameter for the linear regression was set to $12(\frac{n}{100})^{0.25}$, suggested by [35]. Figure 1 displays the count series for part of one single-neuron recording where black color indicates epochs that were classified as stationary.

From the longest stationary spike train of each neuron, we collected all ISIs and estimated their distribution. An example histogram of event intervals is illustrated in Fig. 2 together with model fits of the log-normal (red) and the centralized gamma distribution (blue; for details on the goodness of fit, refer to Sec. IV). If the spiking process was renewal, an adequate formal model of the ISI distribution would suffice to define the renewal model. However, we found that the assumption of independent intervals was violated in the observed spike train of this neuron. This becomes evident in the conditional mean of ISI length in Fig. 2(b), which estimates for all intervals ISI that fall into a given class of interval lengths (bin width 15 ms) the average length of the successive intervals ISI_{i+1}.
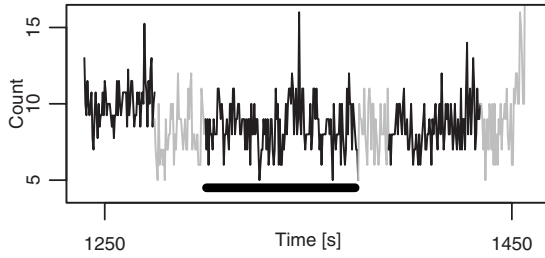
FIG. 1. Test for weak stationarity of the counting process. Spike count of neuron No. 1 observed in successive intervals of 1 s length as a function of time. Gray parts did not deviate significantly from the null hypothesis of a nonstationary time series. Black parts significantly deviated from this null hypothesis and were assumed to be weakly stationary. See text for details on the test procedure.

In general, successive intervals were not independent; in most neurons, we observed a tendency for short intervals to be followed by longer ones and vice versa. This dependence was expressed in a negative Spearman rank-order correlation coefficient [36] of order $p=1$ (calculated for neighboring intervals). This was found to be significant ($P<0.01$, Wilcoxon rank-sum test) in 14 out of 21 neurons (Fig. 3). The example neuron in Fig. 2 exhibited a significant serial correlation of -0.05. The average significant correlation coefficient was -0.15.

Next, we tested for significant higher-order serial correlation of the intervals I_i and I_{i+p}, separated by lag p. We again used Spearman's rank-order correlation coefficient and estimated the partial autocorrelation function (PACF [37]) where for the pth-order correlation we use only every pth data sample. This avoids spurious correlation of order p due to correlations of lower orders $l<p$. We found that none of the spike trains exhibited a significant ($P=0.01$) correlation of higher order $p>1$ and average correlation coefficients close to zero (Fig. 3).

IV. CORRELATED POINT PROCESS MODEL AND PARAMETER ESTIMATION

A linear history-dependent process can be modeled by an autoregressive (AR) process within the limits of stationarity and ergodicity conditions (details are elaborated in [37]). A
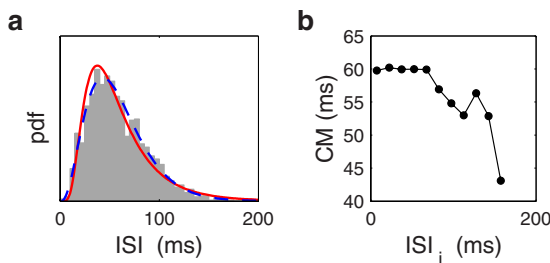

FIG. 2. (Color online) Empirical interspike interval distribution and conditional mean of one MB extrinsic neuron. (a) Histogram of the length of $N=1530$ ISIs (gray). Log-normal (red) and a gamma (dashed blue) model distribution for MLE parameters. (b) Conditional mean (CM) of the $(i+1)$st interval in dependence on the length of the ith interval (estimated in bins of 15 ms).
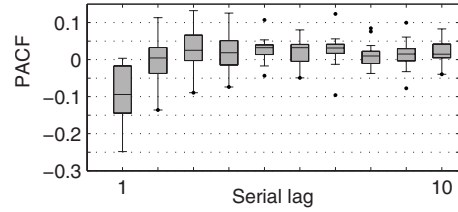

FIG. 3. Partial autocorrelation function for experimentally observed spike trains. Box plots describe the distribution of rank-order correlation across $N=21$ neurons for different serial lags. In 14 cases, the sequence of ISIs exhibited a significant ($P<0.01$) negative correlation of lag 1. For higher lags ($p>1$) the serial correlation did not significantly deviate from 0 ($P=0.01$). Here we tested only neurons with a unimodal shape of the interval distribution.

general form of the autoregressive process with serial dependence up to a finite lag p reads

$$X_s = \beta_1 X_{s-1} + \beta_2 X_{s-2} + \cdots + \beta_p X_{s-p} + \varepsilon_s, \quad (1)$$

where ε_s is assumed to be independent and identically distributed with the specific mean μ and finite variance σ^2. β_i is the correlation parameter for the specific lag i.

Under stationary conditions the distribution of X_s is conditional of the distribution of ε_s. Hence, it is possible to generate surrogate sequences with a specific marginal distribution of interevent intervals. As for the renewal model, the choice of the interval distribution is crucial. It determines to a large extent the count and interval statistics of the process. In practical terms, the model distribution should closely resemble the empiric ISI distribution of the particular neuron type that is to be modeled.

A. Log-normal marginal distribution

In order to modify (1) for generating a series of events consistent with our experimental findings, we need to specify (i) the serial correlation structure and (ii) a marginal interval distribution that describes well our experimental data. With respect to the empirical correlation structure we may simplify the general model (1) to consider only the first-order serial dependence ($\beta=\beta_1$), which we assume to be negative. As a model for the interevent intervals, we chose here the log-normal distribution. This model fits reasonably good to our experimental data (see Fig. 2 and Table II) and leads to a rather simple mathematical description. Thus we have

$$\Delta_s = \exp(X_s) = \exp(\beta X_{s-1} + \varepsilon_s), \quad (2)$$

where ε_s is assumed to be distributed normally with mean μ and variance σ^2, and β describes the negative serial dependence of the series X_s. In fact, the series Δ_s of correlated intervals is the exponential transformation of the series of disturbances X_s. The properties of such transformations of correlated random variables is discussed in great detail in [38].

The mean and variance of X_s are determined by

$$E[X_s] = \frac{\mu}{1-\beta} \quad (3)$$

and

TABLE II. Estimated parameters from experimental spike trains of ten neurons for the autoregressive log-normal and centralized gamma model with first-order serial correlation $\hat{\beta}$. Neurons No. 5 and No. 7 showed a significant ($P=0.05$) deviation from a unimodal distribution.

No.	Log-normal				Centralized gamma				
	$\hat{\mu}$	$\hat{\sigma}$	P^a	$\hat{\beta}$	$\hat{\alpha}$	$\hat{\rho}$	P^a	$\hat{\beta}$	C_V
01	−3.245	1.361	0.090	−0.006	0.797	0.103	0.339	−0.006	1.24
02	−2.239	0.545	**0.000**	−0.268	4.291	0.028	**0.000**	−0.268	0.66
03	−4.628	0.875	**0.011**	0.018	1.581	0.009	**0.028**	0.018	0.88
04	−3.057	0.721	**0.000**	−0.189	2.409	0.024	**0.013**	−0.190	0.61
05	−1.521	1.048	0.759	−0.424	1.129	0.321	0.238	−0.442	0.96
06	−4.232	1.002	**0.000**	−0.103	1.303	0.017	**0.000**	−0.103	0.86
07	−2.974	0.555	**0.013**	−0.062	3.762	0.016	0.477	−0.062	0.51
08	−3.088	1.132	**0.000**	−0.215	1.047	0.075	**0.000**	−0.216	0.96
09	−2.955	0.568	**0.049**	0.007	3.695	0.016	0.780	0.007	0.51
10	−4.077	1.045	**0.013**	−0.068	1.226	0.022	0.222	−0.068	1.06

$^a P$: P-value, Kolmogorov-Smirnov test.

$$V[X_s] = \frac{\sigma^2}{1-\beta^2}, \tag{4}$$

respectively. Thereafter, the expected value of Δ_s is

$$E[\Delta_s] = e^{\mu/(1-\beta)+\sigma^2/2(1-\beta^2)} \tag{5}$$

and its variance is

$$V[\Delta_s] = (e^{2\mu/(1-\beta)+\sigma^2/(1-\beta^2)})(e^{\sigma^2/(1-\beta^2)}-1), \tag{6}$$

and hence the coefficient of variation of this series is

$$C_v[\Delta_s] = \sqrt{e^{\sigma^2/(1-\beta^2)}-1}. \tag{7}$$

The intensity λ for this process can be derived directly from (5) as

$$\lambda = \frac{1}{E[\Delta_s]} = \frac{1}{e^{\mu/(1-\beta)+\sigma^2/2(1-\beta^2)}}. \tag{8}$$

The autocovariance of Δ_s is given in [38], Eq. (2.9).

As we incorporated only the first-order serial correlation β, by iteration over lags we obtain the following:

$$\Delta_s = \exp(X_s) = \exp\left(\sum_{i=0}^{\infty} \beta^i \varepsilon_{s-i}\right). \tag{9}$$

It is evident that the distribution of Δ_s is conditional on the distribution of ε_s if the stationary assumption holds ($|\beta| < 1$). Since the distribution of the ε_s is normal, the distribution of Δ_s is asymptotically log-normal and the series is negatively serially correlated.

Realizations of this autoregressive model are easily obtained by numeric simulation. We performed two example simulations in Fig. 4 where we defined the log-normal interval distribution by the fix mean interval $E[\Delta]=50$ ms and a fix coefficient of variation $C_v[\Delta]=0.5$. The first-order serial correlation parameter was either $\beta=-0.1$ (left) or $\beta=-0.5$ (right). Note that by changing β and keeping $E[\Delta]$ and C_v fixed, we have to adjust σ and μ according to Eqs. (7) and

(5). The empiric interval distributions in Fig. 4(a) (gray histograms) resemble well the model distributions (red). The return maps of the log-transformed ISIs in Fig. 4(c) disclose the negative correlation of neighboring intervals and the empiric estimates of the linear correlation coefficient $\hat{\beta}_i$ of log-transformed intervals closely match the underlying model parameters. The empirical PACFs for serial correlations of lag $p \geq 2$ are close to zero.

B. Generalization of the model

We now propose the generalized gamma density as a more general model for the marginal distribution of Δ_s. For $x > 0$ this can be written as

$$\frac{\Omega}{\Gamma(\alpha)}\left(\frac{1}{\rho}\right)^{\Omega\alpha} x^{\Omega\alpha-1} e^{-(\rho x)^{\Omega}}. \tag{10}$$

This model incorporates some special cases that are widely used to describe experimental ISI distributions of regular spiking neurons. The exponential distribution ($\Omega = \alpha = 1$; e.g., [1,6,32]) describes the well-known special case of a Poisson process with only a single free parameter that determines the mean interval and thus the process intensity. The (centralized) gamma distribution ($\Omega=1$; e.g., [2,20]), the Weibull distribution, and the log-normal distribution (e.g., [39,40]), which describes the limiting case for ($\alpha \to \infty$) have one additional free shape parameter.

Following the same scheme as in (2), we write

$$\Delta_s = \exp(X_s) = \exp(\beta X_{s-1} + \varepsilon_s), \tag{11}$$

where ε_s is assumed to be distributed generalized log-gamma with the vector of parameters

$$\zeta = (\rho, \Omega, \alpha). \tag{12}$$

Since the distribution of ε_s is log-gamma, the distribution of Δ_s will be asymptotically generalized gamma.
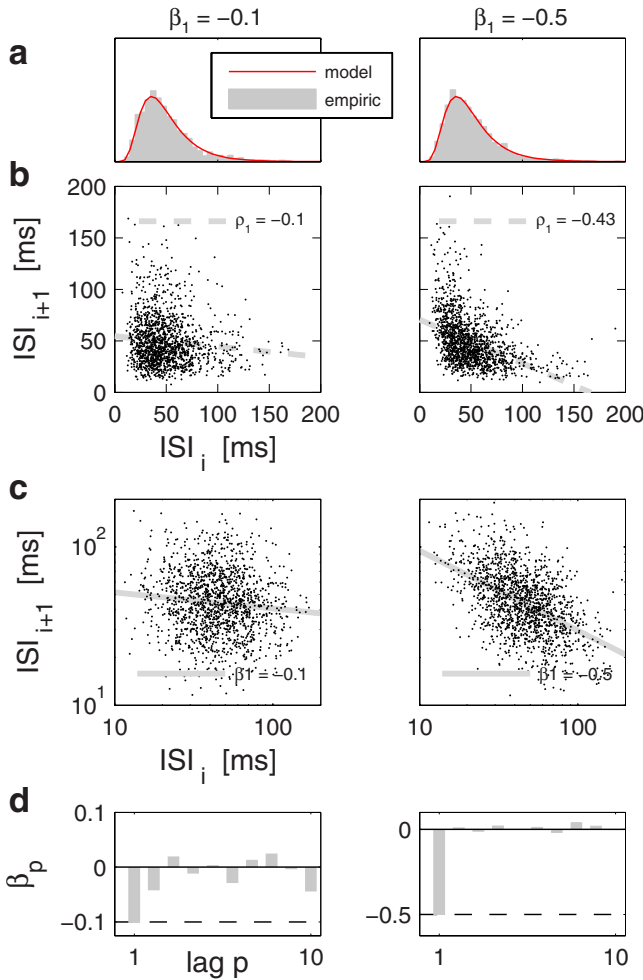
FIG. 4. (Color online) Numeric simulations of the log-normal model. The parameter of first-order serial correlation was set to either $\beta_1 = -0.1$ (left) or $\beta_1 = -0.5$ (right). The parameters of $E[\Delta] = 50$ ms and $C_v = 0.5$ were fixed for both cases. (a) Model (red line) and empiric (gray histogram) interval distribution show a good agreement. (b) Interval return map. The serial dependence of the $(i+1)$st on the ith interval is difficult to see. The linear regression (dashed line) with linear correlation coefficient ϱ_1 of the interval series Δ_s underestimates the correlation parameter β_1. (c) In the interval return map of the log-transformed series $\log(\Delta_s)$ the strong negative correlation is clearly visible (right). The empiric correlation coefficient $\hat{\beta}_1$ is an unbiased estimate of the true correlation β_1. (d) PACFs estimated for serial lags $p \leq 10$.

C. Parameter maximum-likelihood estimation

The model (2) with marginal log-normal distribution has a set of parameters: namely, μ, σ, and β. To obtain a maximum-likelyhood estimator for the parameter set, we re-write the probability density function of the log-normal distribution f_l based on the normal distribution f_N:

$$f_L(\Delta_s; \mu, \beta, \sigma) = \frac{1}{\Delta_s} f_N(\ln \Delta_s; \mu, \beta, \sigma). \tag{13}$$

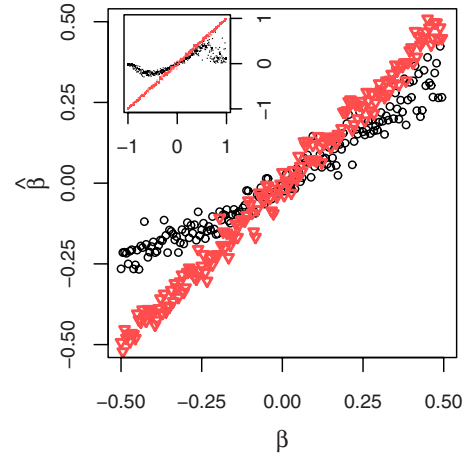Thus, we can write the log-likelihood function of the log-normal distribution (l_L) as

FIG. 5. (Color online) Comparison of linear correlation coefficient (black circles) and MLE estimator for $\hat{\beta}$ (red triangles). Each single estimate is based on a numeric simulation of 10 000 intervals with parameters of neuron No. 1 in Table II. The serial correlation parameter β has been varied in the range $[-0.99, 0.99]$.

$$l_L(\mu, \beta, \sigma | \Delta_1, \Delta_2, \ldots, \Delta_n) = - \sum_k \ln \Delta_k \\ + l_N(\mu, \beta, \sigma | \ln \Delta_1, \ln \Delta_2, \ldots, \ln \Delta_n). \tag{14}$$

Since $\Sigma_k \ln \Delta_k$ is constant with regard to μ, σ, and β, both logarithmic-likelihood functions l_L and l_N reach their maximum with the same μ, β, and σ. Hence, using the expression for the maximum-likelihood estimators (MLEs) for the normal distribution, we can deduce the MLEs for the parameters of the log-normal distribution [33]. The MLEs for the generalized gammamodel are given in [41]. Using the lemma (14), we may obtain the MLEs for the generalized log-gamma distribution. In practical terms, when estimating parameters from a sample $\{\hat{\Delta}\}$ of experimentally obtained intervals, we may first perform a logarithmic transformation and then apply the MLE estimators on the transformed sample $\{\log(\hat{\Delta})\}$.

Maximum-likelihood estimation ensures a bias-free parameter estimation with minimal variance of the estimator. Applying nonoptimal estimators will lead to a biased estimate. The linear correlation coefficient assumes a normal distribution of the random variable and will introduce a bias for log-normal distributed random variables. We illustrate this in Fig. 5 where we simulated realizations of the model described in (2) and subsequently obtained two different estimates $\hat{\beta}$ of the serial interval correlation parameter β. The red triangles in Fig. 5 indicate the estimated values obtained by MLEs on the ordinate which closely match the true parameter values on the abscissa. However, the linear serial correlation coefficient (black circles) strongly underestimates the model inherent serial correlation β with an increasing estimation error for increasing absolute values of β.

D. Empiric estimates of model parameters

In practice, we rarely know for certain that a sample of observed event intervals is drawn from a specific distribu-

tion. Instead, the best we can typically do is to provide evidence that our observations are consistent with a distribution model. A goodness-of-fit test can be performed to assess whether the observations were likely to be drawn from the hypothesized model distribution, which is particularly helpful when choosing between alternative models. We used the Kolmogorov-Smirnov test to assess the goodness of fit of the log-normal and the centralized gamma distribution to the empiric ISI distribution for ten different neurons. In order to perform the test correctly, distribution model parameters were estimated based on the assumed distribution using MLEs. The test results for ten example units are illustrated in Table II. In summery, the test indicates that the model cannot be rejected in approximately 75% and 50% of all neurons for the log-normal and the centralized gamma distribution, respectively ($P \leq 0.01$). Moreover, all units were tested for unimodality based on a test suggested in [42]. Only two neurons showed a significant deviation of their ISI distribution from unimodality (neurons No. 5 and No. 7 in Table II).

V. EFFECT OF SERIAL INTERVAL CORRELATION ON COUNT VARIABILITY

Stochastic point processes are typically described by two inherent stochastic variables. These are the intervals Δ between events and the event count N_T—i.e., the number of events that are expected to fall within a certain time interval of length T. For any given point process, interval and count statistics are closely related. We investigated the effect of serial interval statistics on the variability of the event count in numerical simulations of our model (2). To quantify the count variability we used the Fano factor [14,43] (also "index of dispersion") which normalizes the count variance by the mean count across observations of length T:

$$J_T = \frac{V[N_T]}{E[N_T]}.$$

For renewal models the count variability depends solely on the dispersion of the interval distribution and it holds in the limit of infinite observation that $\lim_{T \to \infty} J_T = C_v^2$ [6,8,44]. This relation will change if the interevent intervals are no longer independent, but exhibit serial dependences. Cox and Lewis [44] derived the following analytic expression for the effect of serial interval correlation of order p on a point process that is otherwise stationary:

$$\lim_{T \to \infty} J_T = C_v^2 \left[1 + 2 \sum_{p=1}^{\infty} \xi_p \right], \quad (15)$$

where ξ_p denotes the autocorrelation function of the interval sequence (i.e., the pth-order linear correlation coefficient) [44]. Using our model (2), we explored the Fano factor as a function of first-order serial interval correlation β in numeric simulations. We again fixed the parameters of mean interval μ and the C_v. For each parameter value of β, we then generated 10 000 point process realizations and computed the Fano factor across all repetitions. Our results in Fig. 6(a) show that J increases with increasing values of *positive* serial correlation, while it decreases with increasing strength of
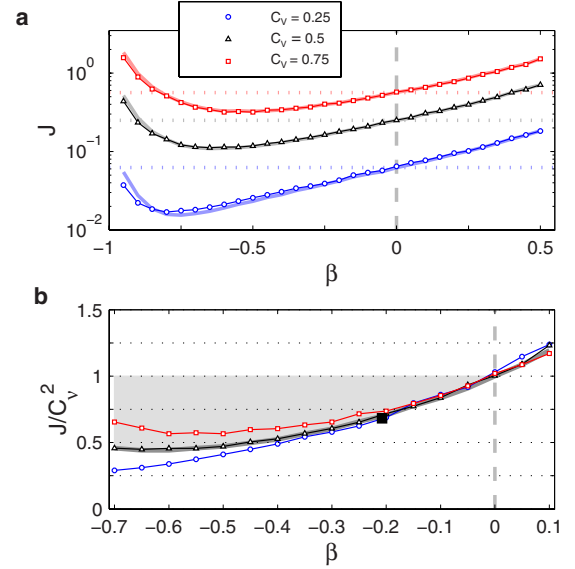

FIG. 6. (Color online) Effect of serial interval correlation on spike count variability. We obtained numerical spike train realizations using our model (2). We varied the serial correlation parameter β and adjusted the parameters (μ, σ) to obtain a fixed value of C_v. (a) Fano factor (J) as a function of β for three different values of C_v as indicated. The horizontal dotted lines indicate the expectation $J = C_v^2$ for a renewal process. The vertical dashed line represents the renewal model where $\beta = 0$. (b) Ratio of J and C_v^2. For the physiologically relevant range with negative first-order serial correlation $\beta \in [-0.5, -0.1]$ (cf. Table I), the Fano factor is clearly smaller than the C_v^2 (gray shaded area). For the renewal model ($\beta_1 = 0$) we find $J / C_v^2 \approx 1$ as expected. Each data point represents 10 000 trials. Each trial comprised on average 100 spikes; this number is sufficiently large to avoid a significant bias of estimation for Fano factor and C_v^2 [14]. The black square reproduces the results given in [24] as the average for seven cortical neurons with significant first-order serial correlation of ISIs (see Discussion).

negative correlation, up to a certain minimum. Our numerical predictions (open symbols) fit well to the analytic prediction (15), which is based on estimates of the linear correlation coefficients ξ_p, again from numerical realizations of our model. In Fig. 6(b) we directly explored the ratio J / C_v^2. It emphasizes the effect of serial correlation on count variability in comparison to the renewal case for which $J \approx C_v^2$. We conclude that the process (2) with a realistic negative correlation strength in the experimentally observed range of $\beta \in [-0.5, -0.1]$ (cf. Table I) exhibits a count variance that is up to 50% *smaller* than predicted from the renewal model.

VI. DISCUSSION

We report here a negative first-order serial correlation of ISIs in the spontaneous activity of mushroom body extrinsic neurons in the honeybee. The estimated negative correlation was generally weak, but significant in the majority of units. Short-lived serial interval correlations have been previously observed in the spontaneous activity of various different types of neurons and with different correlation strengths up to approximately -0.5 for neighboring intervals, as summa-

rized in Table I. This indicates that the spiking processes of those neuron types generally exhibit a nontrivial dependence on the spiking history. In other words, the dynamics underlying a neuron's spike generation is not reset after each spike as is assumed in the prominent renewal model as well as in many computational single-neuron models.

A. Effect of spike sorting errors

Why are there so few reports on the negative interval correlation in the activity of single neurons in central brain structures (cf. Table I)? One possible explanation is the general nonstationary nature of spiking activity in the living brain where firing rates are modulated on different time scales. This generally introduces positive serial correlations that can mask negative interval correlations. A second explanation applies to very low firing rates. In the limit of zero firing rate, all point processes will converge to a Poisson process [26] and thus serial dependences become extinct. If the spike train shows a sufficient degree of stationarity and if the firing frequency is not very low, however, there is one more plausible explanation. Potential errors during the procedure of spike sorting in extracellular recordings may lead to the false assignment of individual spikes to one single unit (false positive spikes) or to missed spikes of one neuron (false negative spikes). Both types of errors will reduce the strength and significance of the empircial correlation measure (simulations not shown) [75] . In practice, spike-sorting errors are inevitable and abundant. E.g., the rate of false positive assignment has been estimated to reach $\approx 10\%$ in the neocortex and a similar number of spikes of a particular neuron are likely to be missed (e.g., [45,46]). This can readily explain why the phenomenon of serial interval correlation has been largely overlooked in *in vivo* preparations where single-neuron activity is accessible mainly through extracellular recording techniques, in particular in the awake animal. Conversely, if we assume that neurons of a certain class do exhibit a particular serial correlation pattern, we might be able to exploit this knowledge in the context of a spike-sorting procedure. In particular, we suggest here to use the significance of the observed first-order negative serial correlation of a putative single unit as a *post hoc* quality measure for the success of the spike sorting algorithm. This will require the continuous measurement of stationary spontaneous activity during parts of the experiment.

B. Cause of negative serial interval correlation

The feature of negatively correlated intervals is likely to be a neuron intrinsic property caused by the same cellular mechanisms that underlie spike frequency adaptation (SFA). The combinatorial effect of calcium influx associated with action potential generation, slow decaying intracellular calcium dynamics, and a calcium-dependent potassium current mediates the so-called slow afterhyperpolarization (e.g., [47–52]). Benda and Herz [53] reviewed the mechanisms underlie the SFA in great detail. In the spontaneous state, this adapting mechanism may lead to an alteration of short and long intervals. Conversely, significant anticorrelation of neighboring intervals in experimental spike trains is indica-

tive of SFA [52] and measures of negative serial correlation may be applied to actually collect evidence for SFA in recordings from awake animals. However, one cannot exclude the possibility that the statistics of the synaptic input under spontaneous conditions causes or alters the serial statistics of the output spike train. For example, in the primary afferent neurons of the electrosensors in the paddle fish, serial correlation of alternating sign exists up to very high serial orders [18,54,55]. This is due to an oscillatory input from hair cells that couples to a second neuron intrinsic oscillator. In an aged preparation where the primary afferent is devoid of its input and thus decoupled from the afferent oscillation, higher-order correlations rapidly decay except for the strong negative first-order correlation, which is caused by neuron intrinsic properties [55].

C. Computational models

We briefly discuss existing models at different levels of abstraction that have been shown to reproduce the experimentally observed negative serial correlation. The choice of a model at the appropriate level of complexity obviously depends on the specific questions under study [56]. Zacksenhouse *et al.* [57] devised a compartmental model of the principal cells of the mammalian lateral superior olive (LSO). Only the inclusion of Ca^{2+}-dependent K^+ channels could reproduce a negative serial dependence of neighboring ISIs that resembled those observed in *in vivo* single-unit recordings from the LSO of an anesthetized cat [22]. In the same issue, Wang [51] presented a biophysical model of a cortical pyramidal neuron with one single dendritic and a somatic compartment. Incorporation of a voltage gated Ca^{2+} conductance and a Ca^{2+}-dependent K^+ conductance produced a pronounced SFA behavior and negative serial correlation of successive intervals for stationary input conditions. The model predicted that the strength of the negative correlation increases with the output firing rate. This has recently been confirmed in an experimental *in vitro* preparation [25] and quantitative prediction for the average correlation coefficient of -0.3 was well met by the recent experimental estimates listed in Table I.

Using a generalized leaky integrate and fire (IF) model with spike frequency adaptation, Liu and Wang [52] predicted values for negative serial interval correlations in cortical pyramidal neurons, again in the range of -0.19 to -0.24. Recently, Muller *et al.* [58] presented a conductance-based IF model with SFA. The neuron, when driven by excitatory and inhibitory synaptic input, reproduces negative serial interval correlation, the strength of which is rate dependent. This model can be reduced to a Markov process for spike-frequency-adapting neural ensembles by adiabatic elimination of fast variables [58]. This elegant approach synthesizes existing mean adaptation approaches, population density methods, and inhomogeneous renewal theory, resulting in a unified and tractable framework which goes beyond renewal and mean-adaptation theories by accounting for correlations between subsequent interspike intervals.

At the next level of reduced complexity, the classic IF model has been modified to produce negative interval corre-

lations by numerical simulation. Introducing a dynamic fatigue of the spike threshold that decays exponentially with physical time introduces a threshold memory [17,59–62]. The maximal order and strength of significant serial correlations is then rate dependent. This model finds analytic treatment in [63]. A simpler modification of the IF model [64] assumes a threshold memory of fixed serial order k and thus produces negative serial correlations only up to order k, independent of the rate.

D. Point process models

Point processes represent a different category of abstract models. They do not provide a complete model of the single neuron as an input-output system. In the mathematical definition, the point process intensity is a predescribed deterministic or stochastic function that describes the time dependence of the event rate—i.e., of the neuron's *output*. Synaptic input *per se* does not find its analogy in these models. However, so-called cascade models (cf. [56]) combine an input stage that converts synaptic drive into an intensity variable with a random point process that generates the spike output. The merits of a stochastic point process model are its analytic formulation and a highly efficient numeric simulation.

We presented a simple autoregressive (AR) point process model that may be seen as a straightforword extension of the widely used renewal model and earlier interval models with serial dependences [65,66]. Our approach models a linear AR process that draws random disturbances ϵ where the distribution of the random variable ϵ is represented on a logarithmic scale (e.g., the log-gamma distribution). We then exponentially transform the resulting sequence to obtain the final sequence of non-negative intervals (e.g., gamma model). The experimentally observed single-unit spike trains showed in all but two cases an unimodal interval distribution that in many cases could be well fitted by a log-normal or centralized gamma distribution (cf. Table II). Our model can be generalized for any well-defined interval distribution [67]. The linear serial correlation coefficients up to finite lag p directly enter our model (2). Empiric estimates of the parameters β_i are obtained using appropriate ML estimators based on a concrete model distribution. An alternative model-free and reliable estimator is provided by Spearman's rank-order correlation coefficient ([36,68]; cf. Fig. 3) which replaces the real-valued intervals by their rank among all intervals which are assumed to be uniformly distributed. Its disadvantage in comparison to the appropriate ML estimator is expressed in the reduced power of the significance test [69]. For our model we apply the PACF to estimate the serial correlation parameters. This requires a sample size that increases only linearly with serial correlation order p and allows for parameter estimation from realistic experimental sample sizes.

A more general approach for generating a history-dependent sequence of intervals rests on the conditional probability density function of an interval given the lengths of the previous intervals as it is described in [7]. This approach of formulating a point process model with serial correlations up to a lag p requires a model of the full p-dimensional interval distribution, or likewise, the p-dimensional hazard term. The difficulty of this approach obviously lies in the empiric estimate of the distribution parameters from experimental data. The number of intervals that is required for a faithful estimate will generally increase exponentially with the power of $p+1$.

The formulation of the conditional intensity function [70] provides a rather general framework to relate the intensity of a point process to its event history and other covariate functions such as the intensity and spiking history of parallel processes [71]. However, empiric estimation of the conditional intensity function typically requires a large amount of experimental data.

E. Reduced single-neuron discharge variability

The variability of the single-neuron discharge across repeated observations, as quantified by the Fano factor, has been extensively studied in various experimental systems. It may be interpreted as noise with respect to the signal encoded in the single neuron's firing rate, which is implicitly assumed to be identical in all experimental repetitions. In point process theory interval and count statistics are directly related. In the renewal case the variance of the interval distribution fully determines the variance of the spike count. Numeric simulations of our nonrenewal model predict that the variability of single-neuron discharge is smaller than expected under the renewal assumption for all neurons that show the typical feature of a negative serial interval correlation in their spontaneous activity. Experimental findings confirm this model prediction. Under spontaneous conditions, the P-type receptor of the weakly electric fish produce regular spike trains with a strong first-order negative serial correlation [16,17]. This resulted in a Fano factor that was much smaller than predicted under the renewal assumption—i.e., for a random permutation of the empiric interval series [17]. We could show elsewhere [24] that cortical spike trains *in vivo* exhibited a negative serial interval correlation with an average strength of $\hat{\beta} \approx -0.2$. This leads to a Fano factor that was about 30% smaller than the C_v^2, which matches well our numerical calibration in Fig. 6. Positive serial correlations of interspike intervals, as, e.g., induced through short- and long-ranged autocorrelation of the input noise to a neuron, increase the Fano factor [72,73]. In physiological terms, such a temporal noise correlation may be interpreted as weak modulation of the background input to a neuron, which results in a subsequent modulation of the output firing rate [14] and hence in positive correlations of the ISIs. Such modulations, however, may easily violate the condition of weak stationarity where we assume a constant mean interval.

The effect of a reduced count variability for negative serial interval correlation is naturally also expressed in the spectral analysis of a spike train. Under stationary conditions, the negative serial correlation reduces the power of the noise spectrum at low frequencies, which enhances the information transfer in the low-frequency domain [18,63,64]. This noise-shaping effect was confirmed in experimental data from the P-type receptor of the weakly electric fish [74]. Note that this effect diminishes at high frequencies. This frequency dependence is equally expressed in the dependence

of the Fano factor on the length T of the observation interval. For shorter intervals the Fano factor tends to unity, $\lim_{T \to 0} J_T = 1$, while the C_v tends to zero, independent of the stochastic nature of the underlying process [14].

As discussed before, we may expect that erronous spike sorting has frequently led to the analysis of "single-unit activity" that was not 100% single-neuron activity. If we assume a negative interval correlation in the single-neuron activity, we may deduce two major effects of spike sorting errors on the statistics of the sorted unit activity [75]: (a) The Fano factor increases when serial correlation diminishes, and (b) the variance of the interval length (C_v) likely increases due to false positive and false negative spikes that truncate or merge the original spike trains with a biased production of too short and too long intervals. We may speculate that spike sorting errors lead to a systematic over estimation of count and interval variability, and thus may have caused a biased picture of single-neuron variability. We believe that a cautious reevaluation of serial spike train statistics and of spike count variability is necessary particularly in the *in vivo* activity of central neurons. As we have discussed elsewhere [14], additional factors may lead to an overestimation of the true single-neuron variability in experimental recordings from awake animals. In central brain structures the most prominent influence is to be expected from ongoing activity that is not directly related to the experimental task under observation [76–78].

As outlined above, we hypothesize that the large class of neurons that feature an intrinsic SFA mechanism generally exhibit a negative serial correlation under spontaneous conditions. We may thus formulate the working hypothesis that the SFA mechanism reduces count variability not only under spontaneous conditions, but generally also under response

conditions. This would result in a more reliable transmission of an input signal in favor of a rate code and might improve stimulus decoding in downstream neurons. Along these lines, Chacron *et al.* could show that the noise shaping due to the nonrenewal spike train structure in the population of afferent receptor neurons improved stimulus representation in postsynaptic cells [74]. Lüdtke and Nelson demonstrated in a model study that postsynaptic neurons can directly exploit the nonrenewal structure of a presynaptic spike train and benefit from an enhanced sensitivity to weak signals on a noisy background [62].

F. Open-source tools

We provide implementations of various tools for numeric point process simulation and parameter estimation within the FIND open-source toolbox for neural data analysis with Matlab [79] (http://find.bccn.uni-freiburg.de/). Implementations in Python will be made available at the portal site of G-Node [80] (www.g-node.org), the German node of the International Neuroinformatics Coordinating Faciles (INCF).

ACKNOWLEDGMENTS

[1] G. L. Gerstein and B. Mandelbrot, Biophys. J. **4**, 41 (1964).
[2] R. B. Stein, Biophys. J. **7**, 37 (1965).
[3] G. O. Moore, D. Perkel, and J. Segundo, Annu. Rev. Physiol. **28**, 493 (1966).
[4] D. H. Perkel, G. L. Gerstein, and G. Moore, Biophys. J. **7**, 391 (1967).
[5] D. H. Perkel, G. L. Gerstein, and G. Moore, Biophys. J. **7**, 419 (1967).
[6] H. C. Tuckwell, *Introduction to Theoretical Neurobiology* (Cambridge University Press, New York, 1988).
[7] D. H. Johnson, J. Comput. Neurosci. **3**, 275 (1996).
[8] D. R. Cox, *Renewal Theory* (Methuen, London, 1962).
[9] M. J. Berry and M. Meister, J. Neurosci. **18**, 2200 (1998).
[10] D. S. Reich, J. D. Victor, and B. W. Knight, J. Neurosci. **18**, 10098 (1998).
[11] R. E. Kass and V. Ventura, Neural Comput. **13**, 1713 (2001).
[12] R. Barbieri, M. C. Quirk, L. M. Frank, M. A. Wilson, and E. N. Brown, J. Neurosci. Methods **105**, 25 (2001).
[13] E. N. Brown, R. Barbieri, V. Ventura, R. E. Kaas, and L. M. Frank, Neural Comput. **14**, 325 (2001).
[14] M. P. Nawrot, C. Boucsein, V. R. Molina, A. Riehle, A. Aertsen, and S. Rotter, J. Neurosci. Methods **169**, 374 (2008).
[15] L. Devroye, *Non-uniform Random Variate Generation* (Springer-Verlag, New York, 1986).
[16] R. Ratnam and M. Nelson, J. Neurosci. **20**, 6672 (2000).
[17] M. J. Chacron, A. Longtin, M. St-Hilaire, and L. Maler, Phys. Rev. Lett. **85**, 1576 (2000).
[18] A. B. Neiman and D. F. Russell, J. Neurophysiol. **92**, 492 (2004).
[19] M. W. Levine, Biophys. J. **30**, 9 (1980).
[20] S. W. Kuffler, R. Fitzhugh, and H. B. Barlow, J. Gen. Physiol. **50**, 683 (1957).
[21] R. W. Rodieck, J. Neurophysiol. **50**, 1044 (1967).
[22] C. Tsuchitani and D. H. Johnson, J. Acoust. Soc. Am. **77**, 1484 (1985).
[23] M. A. Lebedev and R. J. Nelson, Exp. Brain Res. **111**, 313 (1996).
[24] M. P. Nawrot, C. Boucsein, V. Rodriguez-Molina, A. Aertsen, S. Grün, and S. Rotter, Neurocomputing **70**, 1717 (2007).
[25] T. Engel, L. Schimansky-Geier, A. Herz, S. Schreiber, and I. Erchova, J. Neurophysiol. **100**, 1576 (2008).
[26] M. J. Chacron, B. Lindner, and A. Longtin, J. Comput. Neurosci. **23**, 301 (2007).
[27] K. Floyd, V. H. Hick, A. Holden, J. Koley, and J. B. Morrison,

Biol. Cybern. **45**, 89 (1982).

[28] R. Menzel, Learn. Memory **8**, 53 (2001).

[29] G. M. R. Okada, J. Rybak, and R. Menzel, J. Neurosci. **27**, 11736 (2007).

[30] M. F. Strube-Bloss, Ph.D. thesis, Free University of Berlin, 2008.

[31] J. Rybak and R. Menzel, J. Comp. Neurol. **334**, 444 (1993).

[32] D. H. Perkel, G. L. Gerstein, and G. Moore, Biophys. J. **7**, 391 (1967).

[33] J. Johnston and J. Dinardo, *Econometric Methods* (McGraw-Hilll, Singapore, 1954).

[34] P. C. B. Phillips and P. Perron, Biometrika **75**, 335 (1988).

[35] A. Trapletti and K. Hornik, Computer code TSERIES, r package version 0.10-11., URL http://CRAN.R-project.org/.

[36] M. Kendall, *Rank Correlation Methods* (Griffin, London, 1962).

[37] P. J. Brockwell and R. A. Davis, *Time Series: Theory and Methods* (Springer, New York, 1991).

[38] C. W. J. Granger and P. Newbold, J. R. Stat. Soc. Ser. B (Methodol.) **38**, 189 (1976).

[39] B. D. Burns and A. C. Webb, Proc. R. Soc. London, Ser. B **194**, 211 (1976).

[40] M. W. Levine, Biol. Cybern. **65**, 459 (1991).

[41] E. Ortega, H. Bolfarine, and G. Paula, Comput. Stat. Data Anal. **42**, 165 (2003).

[42] J. A. Hartigan and P. M. Hartigan, Ann. Stat. **13**, 70 (1985).

[43] U. Fano, Phys. Rev. **72**, 26 (1947).

[44] D. R. Cox and P. A. W. Lewis, *The Statistical Analysis of Series of Events*, Methuen's Monographs on Applied Probability and Statistics (Methuen, London, 1966).

[45] M. Joshua, S. Elias, O. Levine, and H. Bergman, J. Neurosci. Methods **163**, 267 (2007).

[46] C. Pouzat, M. Delescluse, P. Viot, and J. Diebolt, J. Neurophysiol. **91**, 2910 (2004).

[47] P. Pennefather, B. Lancater, P. R. Adams, and R. A. Nicoll, Proc. Natl. Acad. Sci. U.S.A. **82**, 3040 (1985).

[48] D. A. McCormick and A. Williamson, Proc. Natl. Acad. Sci. U.S.A. **86**, 8098 (1989).

[49] M. V. Sanchez-Vives, L. G. Nowak, and D. A. McCormick, J. Neurosci. **20**, 4286 (2000).

[50] A. Tzingounis, M. Kobayashi, K. Takamatsu, and R. Nicoll, Neuron **53**, 487 (2007).

[51] X.-J. Wang, J. Neurophysiol. **79**, 1549 (1998).

[52] Y. Liu and X. Wang, J. Comput. Neurosci. **10**, 25 (2001).

[53] J. Benda and A. V. M. Herz, Neural Comput. **15**, 2523 (2003).

[54] A. Neiman and D. F. Russell, Phys. Rev. Lett. **86**, 3443 (2001).

[55] A. B. Neiman and D. F. Russell, Phys. Rev. E **71**, 061915 (2005).

[56] A. V. M. Herz, T. Gollisch, C. K. Machens, and D. Jaeger, Science **314**, 80 (2006).

[57] M. Zacksenhouse, D. Johnson, J. Williams, and C. Tsuchitani, J. Neurophysiol. **79**, 3098 (1998).

[58] E. Muller, L. Buesing, J. Schemmel, and K. Meier, Neural Comput. **19**, 2958 (2007).

[59] M. J. Chacron, A. Longtin, and L. Maler, J. Neurosci. **21**, 5328 (2001).

[60] R. Brandman and M. E. Nelson, Neural Comput. **14**, 1575 (2002).

[61] M. Zacksenhouse, D. Johnson, J. Williams, and C. Tsuchitani, Neural Comput. **15**, 253 (2003).

[62] N. Lüdtke and M. E. Nelson, Neural Comput. **18**, 2879 (2006).

[63] B. Lindner, M. J. Chacron, and A. Longtin, Phys. Rev. E **72**, 021911 (2005).

[64] M. J. Chacron, B. Lindner, and A. Longtin, Phys. Rev. Lett. **92**, 080601 (2004).

[65] H. Wold, *A Study in Analysis of Stationary Time Series* (Almquist and Wiksell, Stockholm, 1954).

[66] D. P. Gaver and P. A. W. Lewis, Adv. Appl. Probab. **12**, 727 (1980).

[67] N. G. V. Kampen, *Stochastic Processes in Physics and Chemistry* (Elsevier, Amsterdam, 2007).

[68] W. H. Press, S. A. Teukolsky, W. T. Vetterling, and B. P. Flannery, *Numerical Recipes in C*, 2nd ed. (Cambridge University Press, Cambridge, England, 1992).

[69] E. L. Lehmann, Ann. Math. Stat. **24**, 23 (1953).

[70] D. Daley and D. Vere-Jones, *An Introduction to the Theory of Point Processes* (Springer-Verlag, New York, 2007).

[71] W. Truccolo, U. T. Eden, M. R. Fellows, J. P. Donoghue, and E. N. Brown, J. Neurophysiol. **93**, 1074 (2005).

[72] J. W. Middleton, M. J. Chacron, B. Lindner, and A. Longtin, Phys. Rev. E **68**, 021920 (2003).

[73] T. Schwalger and L. Schimansky-Geier, Phys. Rev. E **77**, 031914 (2008).

[74] M. J. Chacron, L. Maler, and J. Bastian, Nat. Neurosci. **8**, 673 (2005 May).

[75] M. Nawrot, C. Boucsein, S. Grün, and F. Farkhooi in *The 4th Bernstein Symposium for Computational Neuroscience* (Frontiers Research Foundation, Lausanne, in press).

[76] A. Arieli, A. Sterkin, A. Grinvald, and A. Aertsen, Science **273**, 1868 (1996).

[77] D. Leopold, Y. Murayama, and N. Logothetis, Cereb. Cortex **13**, 422 (2003).

[78] M. P. Nawrot, Ph.D. thesis, Albert-Ludwigs-University Freiburg, Germany, 2003.

[79] R. Meier, U. Egert, A. Aertsen, and M. P. Nawrot, Neural Networks **21**, 1085 (2008).

[80] A. V. Herz, R. Meier, M. Nawrot, W. Schiegel, and T. Zito, Neural Networks **21**, 1070 (2008).